

RITA: Boost Autonomous Driving Simulators with Realistic Interactive Traffic Flow

Zhengbang Zhu^{*1}, Shenyu Zhang^{*1}, Yuzheng Zhuang^{*2}, Yuecheng Liu², Minghuan Liu¹,
Liyuan Mao¹, Ziqing Gong¹, Weinan Zhang¹, Shixiong Kai², Qiang Gu²,
Bin Wang², Siyuan Cheng², Xinyu Wang³, Jianye Hao² and Yong Yu¹
¹ Shanghai Jiao Tong University, ² Noah's Ark Lab, Huawei Technologies Co.,Ltd.
³ IAS BU ADS Planning and Control, Huawei Technologies Co.,Ltd.

China

{zhengbangzhu,zsyofficial,minghuanliu,maoliyuan,gongzq0301,wnzhang,yyu}@sjtu.edu.cn
{zhuangyuzheng,liuyuecheng1,kaishixiong,qiang.gu,wangbin158,chengsiyuan8,wangxinyu8,haojianye}@huawei.com

ABSTRACT

High-quality traffic flow generation is the core module in building simulators for autonomous driving. However, the majority of available simulators are incapable of replicating traffic patterns that accurately reflect the various features of real-world data while also simulating human-like reactive responses to the tested autopilot driving strategies. Taking one step forward to addressing such a problem, we propose Realistic Interactive Traffic flow (RITA) as an integrated component of existing driving simulators to provide high-quality traffic flow for the evaluation and optimization of the tested driving strategies. RITA is developed with fidelity, diversity, and controllability in consideration, and consists of two core modules called RITABackend and RITAKit. RITABackend is built to support vehicle-wise control and provide traffic generation models from real-world datasets, while RITAKit is developed with easy-to-use interfaces for controllable traffic generation via RITA-Backend. We demonstrate RITA's capacity to create diversified and high-fidelity traffic simulations in several highly interactive highway scenarios. The experimental findings demonstrate that our produced RITA traffic flows meet all three design goals, hence enhancing the completeness of driving strategy evaluation. Moreover, we showcase the possibility for further improvement of baseline strategies through online fine-tuning with RITA traffic flows.

KEYWORDS

Micro Traffic Generation, Imitation Learning, Autonomous Driving

ACM Reference Format:

Zhengbang Zhu^{*1}, Shenyu Zhang^{*1}, Yuzheng Zhuang^{*2}, Yuecheng Liu², Minghuan Liu¹, Liyuan Mao¹, Ziqing Gong¹, Weinan Zhang¹, Shixiong Kai², Qiang Gu², Bin Wang², Siyuan Cheng², Xinyu Wang³, Jianye Hao² and Yong Yu¹. 2023. RITA: Boost Autonomous Driving Simulators with Realistic Interactive Traffic Flow. In *Proc. of the 22nd International Conference on Autonomous Agents and Multiagent Systems (AAMAS 2023)*, London, United Kingdom, May 29 – June 2, 2023, IFAAMAS, 13 pages.

* The authors contributed equally.

1 INTRODUCTION

With the empowered ability of artificial intelligence, autonomous driving has become one of the promising directions for both research and application. Due to the safety concern and the high cost of real vehicle testing, autopilot simulation is widely used for fast iteration and verification of driving algorithms [15, 31]. It attracts massive attention from researchers and industries to build a high-quality simulator. However, existing open-sourced autopilot simulators primarily focus on traffic modeling with hand-scripted rules to facilitate lane following, collision avoidance, etc. [17, 25]. Such heuristic rules are insufficient to model the variability and noise in real-world human driving behaviors.

To improve the fidelity of driving behavior simulation, replaying the movement in the human driving dataset [30] has become popular. However, the data replay lacks fidelity during real-time interactions, since the social vehicles cannot provide reasonable responses when the ego vehicle acts differently as in the dataset. To further generate both realistic and reactive traffic flows, supervised learning approaches have been applied in social vehicle modeling [2, 3]. Unfortunately, supervised decision models suffer from compounding errors [40] and causal confusion [13] problems, which make them perform poorly as the planning steps and traffic density increase. Adversarial imitation learning methods handle these issues through rich online interactions in driving simulators [7, 8]. However, few works have explored the potential of using them to enhance the traffic flow in existing simulators.

Another advantage of using simulations is that it allows users to design extensive and specific scenarios beyond those from the datasets to evaluate driving strategies. Prior learning-based works in building traffic flow only use a single model or multiple models separately [24, 43], which limits the configurability of the simulator. A recent work, SimNet [3], replaces the model-inferred steering angle with hard-coded values to force generating lane-changing behaviors of social vehicles. This approach sacrifices fidelity to provide specific interaction scenarios. Instead, our focus is to enable specific scenario generations while maintaining fidelity.

To provide a principled and unified solution for building high-quality traffic flows in autonomous driving simulators, in this paper, we propose RITA, a traffic generation framework with Realistic Interactive Traffic flow. RITA focuses on augmenting existing autonomous driving simulators with high-quality traffic flows, aiming

at reaching three design goals: *fidelity*, *diversity*, and *controllability*. To meet these requirements, RITA is developed with two core modules: RITABackend and RITAKit. The first module, RITABackend, incorporates machine learning models built from real-world datasets, including vehicle control and guided traffic generation models. In particular, the vehicle control models are trained using adversarial imitation learning methods, which generate specific behaviors and generalize better outside the data distribution than supervised methods. In addition, the guided traffic generation models are for customized background traffic generation, providing specific initialization states with a guided diffusion sampling algorithm. The second module, RITAKit, is an easy-to-use toolkit that combines models from RITABackend to generate traffic flows in the simulator. RITAKit has a friendly programming interface that makes it easy to set up the different traffic flows that can be controlled.

To show the superiority of generated traffic flows and demonstrate the usages of RITA, we conduct experiments on two representative tasks in highway driving, *cut-in* and *ramp*. With regard to these tasks, we first assess the quality of the generated traffic flow with regard to three design goals. Then we show two use cases of RITA to facilitate the autonomous driving workflow. On the one hand, RITA traffic flow can be used flexibly to benchmark off-the-shelf driving strategies from different aspects. Benchmarked driving strategies are either hand-crafted or trained with the history-replay traffic flow. Also, RITA traffic flow can help further improve the driving strategies’ performances by allowing online interactions with reactive and realistic social vehicles. Currently, RITA is in the process of being incorporated into Huawei’s autonomous driving platform. In the future, we hope RITA can serve as a standard building block in developing high-fidelity autonomous driving simulators and contribute to the evaluation and improvement of driving strategies for the community.

2 KEY FEATURES

We highlight three key features of the traffic flow in RITA.

Fidelity. Fidelity is an essential measure of simulators that describes the gap between the simulation and the reality [42]. In particular, driving simulators are essential for ensuring the sim-to-real performance of driving algorithms and are the most effective evaluation tool before real-world road testing. Thus, the smaller the gap between the interaction responses in the simulator and those encountered in reality, the more likely it is that a strategy achieving high performance in the simulator will also perform well in real road conditions. The fidelity of the traffic flow lies in two aspects: 1) the vehicle state distribution in the traffic flow. For example, social vehicles always move fast on highways in light traffic conditions; 2) the fidelity of the responses from the social vehicles when interacting with the ego vehicle, like the typical lane-changing scenario. We observe that human drivers exhibit specific noise in multiple dimensions when performing lane changes in real datasets. Therefore, we would expect that the traffic flows generated by RITA also possess similar microscopic properties to human interaction behaviors.

Diversity. Human driving behavior exhibits a high degree of diversity due to differences in destinations, road conditions, drivers’

personalities, and other factors. This means, in similar situations, three distinct drivers will behave differently: if driver A tries to change lanes to the left when there is a vehicle in his front, driver B can tend to maintain his current route; even if driver C also chooses to change lanes, the timing of action and the speed of lane change can be quite different. To reach that, we must ensure that RITA’s basic vehicle control models include as much behavioral diversity as possible from real data. In addition, when these models are combined to generate diversified traffic flow, the resulting behavior still maintains a high fidelity level.

Controllability. Building upon diversity, we can define controllability as an enhancement feature, i.e., the ability to generate customized traffic flows based on user specifications from many potential instances. For example, we can construct test tasks with different difficulty levels by adjusting the distribution and behavior of the traffic flow, or we can generate scenarios with a targeted assessment of the weaknesses of the driving strategy under test. High controllability also corresponds to high usability, allowing various researchers to build their benchmark tasks by simply changing the parameters of the traffic definition interface in RITAKit. The modular design of RITA allows it to be easily extended to more maps and datasets or even used by other simulators.

3 RITA OVERVIEW

In this section, we present an overview of our proposed traffic generation framework. To achieve the three design goals, the framework needs to be able to have sufficient expressiveness to cover the diverse traffic flows in the real data and enough variable modules to support the generation of specific traffic flows based on the users’ specifications. At a glance, we maintain a diverse zoo of vehicle control models and multiple static replay trajectories generation methods, and propose a set of interfaces for traffic definition to achieve the above requirements.

We start with the general formulation of autonomous driving, and then give a compositional illustration of RITA.

3.1 General Formulation

We consider the autonomous driving task in the discrete-time setting within a fixed roadway area [18, 21, 41], where each vehicle acts simultaneously at each time step and vehicles can enter or drive out of the given area, and therefore causing the number of vehicles to change. Formally, denote the vehicles in the area at each time step t as a set $V_t = \{v_1, v_2, \dots, v_{n_t}\}$, where v_i denotes unique vehicle index, and n_t is the number of vehicles. Then, the simulation proceeds by iterating between every vehicle $v \in V_t$ takes its individual action a_t^v according to some policy $\pi(a_t^v|h_t^v)$ based on its historical observations $h_t^v = (o_0^v, \dots, o_t^v)$, and the simulator updates global state s_t to s_{t+1} under the transition function $\mathcal{T}(s_{t+1}|s_t, \mathbf{a}_t)$, where the joint action $\mathbf{a}_t = [a_i]_{i=1}^{n_t}$ is the concatenation of all vehicles’ actions.

The goal of this paper is to build microscopic traffic flows that can interact with user-specified driving strategies, which are referred to as the *ego strategies* in the following text. Thereafter we divide the vehicles as *ego vehicles* and *social vehicles*. Ego vehicles are those that are controlled by ego strategies, while social vehicles’ movements are determined by the simulator, data replay, or the

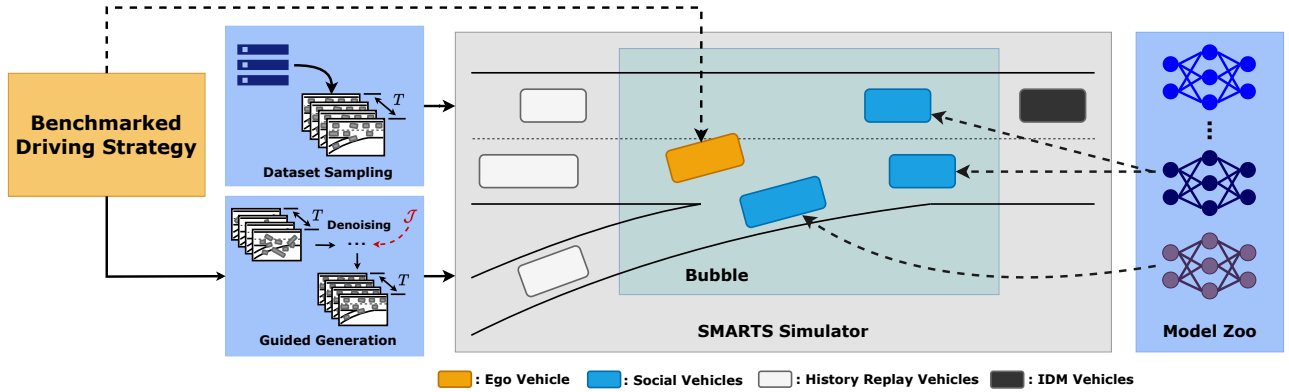


Figure 1: Overview of the RITA traffic generation pipeline.

trained reactive agents as in Section 4. Note that such divisions do not have to be fixed during simulation. For example, one vehicle can be a social vehicle in the first half of an episode and is then taken over by the ego strategies for the second half.

3.2 Compositional Illustration

RITA’s aspiration is to create high-quality traffic flow to improve the existing driving simulators. Developing a simulator and building basic components (such as kinematic simulation, collision detection, etc.) from scratch are outside the major scope of concern. To this end, we choose to build upon an existing simulator, in this paper particularly, SMARTS [43], yet it is feasible to integrate RITA into any other simulators such as SUMO [25] and BARK [5].

In total, RITA can be decomposed into two core modules, RITAKit and RITABackend. As a high-fidelity traffic generation framework, RITA can be initialized from real-world datasets and transform traffic specifications to specific scenarios.

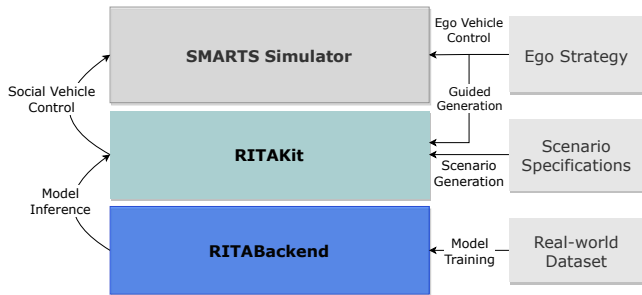


Figure 2: Compositional illustration of RITA.

We illustrate the architecture of RITA in Fig. 2, organized by a bottom-to-top order. First, real-world datasets are used to train machine learning models in RITABackend. Once models are built, the scenarios can be configured via RITAKit with scenario specifications, usually expressed as parameters in a unified traffic generation function. Notably, RITAKit directly operates on RITABackend and transforms scenario specifications into model calls in RITABackend. With this decoupled design, the creation and adjustment of benchmark tasks can be made with less effort, where users do not

need to define each sub-model call manually. During the evaluation procedure, both RITAKit and ego strategies are plugged into SMARTS to control social vehicles and ego vehicles, respectively. RITAKit also takes ego strategies as input for rare-case generation and automatically generates customized traffic flows.

In the following, we further show the training and evaluation results for models in RITABackend in Section 4, and describe RITAKit in detail in Section 5.

4 BUILDING RITABACKEND

4.1 Model Zoo

To evaluate the ego strategies with high-fidelity traffic flows, we mandate a set of reactive agents that can generate traffic flows during flexible interactions. Instead of designing complex and proper reward functions for learning autonomous driving agents, we choose to learn to behave like a human driver from real-world data. To this end, we utilize imitation learning methods [22, 28], which provide a way to learn from demonstrations and mimic the demonstrator’s behaviors. In RITA, we maintain a model zoo that integrate a set of imitation learning algorithms for building reactive agents. There exists some previous methods that take behavior cloning (BC) to learn their reactive agents, such as [2, 4] due to its simplicity. However, BC can suffer from serious compounding error problem when data is limited [32]. On the contrary, inverse reinforcement learning (IRL) methods [1] theoretically outperform BC with less compounding error [40]. Thereafter, we mainly take the off-the-shelf Generative Adversarial Imitation Learning (GAIL) algorithm [22] and its variants in our model zoo. As a popular online imitation learning algorithm induced from the IRL framework, GAIL inherits the advantage in less compounding error and has been successfully applied in driving behavior imitation [26]. In the sequel, we briefly introduce these methods and their features for strategy learning.

4.1.1 Single-agent GAIL. Although GAIL is designed to solve imitation learning problems for a single agent, we can apply it to multi-agent learning problems by independently learning different agents’ strategies. In our implementation, we train the policy models of each agent by replacing certain history vehicles in the replay data as the ego vehicle to be controlled. Using hand-scripted rules to select expert data with specific interactive behavior (e.g.,

left cut-in), we can ask the trained models to have desired reactive and interactive capability.

4.1.2 InfoGAIL. To model the diversity of human driving and produce high-quality interactive scenarios from unlabeled recorded data, we contain InfoGAIL [27] in our model zoo to be a multi-modal reactive agent, which models and controls different distinct modalities of the recorded data with a latent variable. Since InfoGAIL is also a single-agent algorithm, the implementation follows the independent training style as GAIL. We can produce diverse scenarios according to different preferences by controlling the discrete variable. The InfoGAIL agent is also trained on a filtered dataset to serve as a reactive agent for specific behaviors.

4.1.3 MAGAIL. Considering the multi-agent nature of autonomous driving and modeling the interaction between different agents, we also include the multi-agent extension of GAIL, i.e., MAGAIL [35], serving as a multi-agent reactive agent. We want MAGAIL to model a general reactive policy that does not have to make any active interaction to influence the benchmarked strategies to be evaluated but instead makes passive responses only to ensure safe driving. This is implemented using the entire traffic flow dataset. By carrying out the parameter sharing technique [9], MAGAIL controls all the vehicles in an area.

4.2 Model Performance Analysis

To show the high fidelity of the learned models, we evaluate their performance from four aspects:

- **Safety:** Non-collision rate with social vehicles.
- **Completion:** Completion rate of finishing specific interaction behavior.
- **Stability:** A selected constant minus the mean value of acceleration and yaw rate for the trajectory.
- **Diversity:** Standard deviation of acceleration and yaw rate for the trajectory.

The results are shown in Fig. 3. It is easily concluded that all GAIL-based models enjoy high safety and completion rate, which outperforms BC a lot, showing their capability for traffic generalization. The high stability provides smooth driving behavior similar to humans, along with some model-specific character. In particular, we find that the multi-agent reactive agent (MAGAIL) has the highest safety rate while the multi-modal reactive agent (InfoGAIL) differs in diversity. These features indicate the necessity of multiple training algorithms for diverse models. Notably, the model performance does not seem high enough to create totally safe traffic, which may be because we enforce the model to make specific interactive behavior, resulting in the loss of reactivity. However, complete safety is meaningless since autonomous driving simulation needs exactly the realistic but unsafe environment for policy to make self-improvement.

4.3 Guided Traffic Generation

When utilizing RITA to provide traffic flows for interacting with ego vehicles, a natural way is making all social vehicles controlled by reactive agents from the model zoo. However, such an approach can be computationally expensive when there exists a large number of vehicles. Also, when an increasing number of vehicles react to

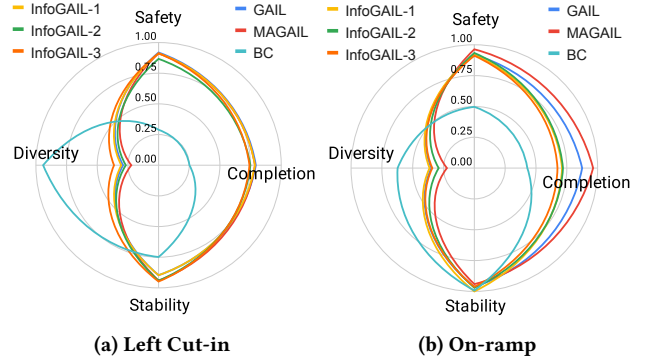


Figure 3: Performance of vehicle control models in the model zoo. We evaluate the performance from four aspects, where Safety and Completion focus on the driving task itself; Stability and Diversity measure the actions in trajectory.

each other, there is a growing chance of deviating from model training distributions. To save simulation cost and alleviate the aforementioned distributional shifts, we pre-specify a special region, which is called *bubble*, on the map. Typically, the bubble covers the area inside which reactive behaviors are mostly expected to happen, such as the ramp merge area. Only social vehicles inside the bubble are controlled by reactive models, while others are just replaying movements in static trajectories. In such a context, these static trajectories profoundly affect the interactions within the bubble by determining the initial states of social vehicles entering it. Even if we fix the control model of social vehicles within the bubble, the performance of ego vehicles under different static trajectories can vary much due to factors such as traffic density and the distance between social vehicles and ego vehicles.

Normally, the static trajectories can be sampled using *dataset sampling*, i.e., directly sampled from datasets. Although dataset sampling maintains a high degree of fidelity, it has a slight chance to sample trajectories from the long tail part of its distribution (e.g., a group of quite dense traffic) as the dataset can be potentially large. Also, the sampled trajectories are agnostic to benchmarked strategies; therefore, dataset sampling overlooks the fact that every strategy has its Achilles heel.

To generate static trajectories with more flexibility and controllability, RITA additionally provides *guided generation* for acquiring static trajectories. First, a diffusion-based generative model s_θ is trained in RITABackend to cover the multi-vehicles trajectories distribution of the dataset. The diffusion model is trained with the same objective as in DDPM, which is a reweighed version of the evidence lower bound (ELBO):

$$\theta^* = \arg \min_{\theta} \sum_{i=1}^N (1 - \alpha_i) \mathbb{E}_{p(x)} \mathbb{E}_{p_{\alpha_i}(\tilde{x}|x)} [\|s_\theta(\tilde{x}, i) - \nabla_{\tilde{x}} \log p_{\alpha_i}(\tilde{x}|x)\|_2^2], \quad (1)$$

where $p(x)$ is the multi-vehicle trajectories distribution in the dataset, $\alpha_i = \prod_{j=1}^i (1 - \beta_j)$, $p_{\alpha_i}(\tilde{x}|x) = \mathcal{N}(\tilde{x}; \sqrt{\alpha_i}x, (1 - \alpha_i)\mathbf{I})$, and $0 < \beta_1, \beta_2, \dots, \beta_N < 1$ is a sequence of positive noise scales.

After training, users can specify a (differentiable) scoring function on trajectories, whose gradient is used for guided sampling

from the diffusion model [36]. A prediction network $\mathcal{J}(x)$ trained on a small labeled dataset is well suited as the scoring function. The generated static trajectories are guided towards the high-score instances while still within the real data support. The reverse diffusion process transitions during guided sampling are sampled from:

$$p_{\theta}^{\mathcal{J}}(x^{i-1}|x^i) = \mathcal{N}(x^{i-1}; \mu + \Sigma \nabla \mathcal{J}(\mu), \Sigma), \quad (2)$$

where μ, σ are the parameters of the original reverse process transition $p_{\theta}(x^{i-1}|x^i)$.

Since it is difficult to define the order of vehicles in a multi-vehicle trajectory, the diffusion model uses a shared U-Net structure to process each vehicle’s trajectory and perform an order-independent self-attention operation on all vehicles’ intermediate features of the last encoder layer. The score function we used shares the same encoder structure with the diffusion model but only performs attention operation between ego vehicle and other vehicles rather than a complete self-attention. This is because the metrics labels we used to train the scoring functions are primarily egocentric.

5 RITAKIT: A CONFIGURABLE TRAFFIC GENERATION TOOLKIT

In this section, we present RITAKit, a traffic flow generation toolkit for interactive scenarios. RITAKit is a middle-ware that connects user specifications and RITABackend to generate traffic flow. From the user perspective, RITAKit is an easy-to-use programming interface, and the following code block shows an example of assigning a user-specific scenario.

```

1 ScenarioMaker(
2     scenario = "ngsim-i80",
3     bubble = Bubble(
4         type='moving',
5         zone=Rectangle(40,20)),
6     interaction = "CommonLeftCutin",
7     guided_generation = "Stability",
8 )

```

We elaborate on each input parameter with how it influences the traffic flow and currently supported options.

- *scenario* specifies the map and the corresponding real-world dataset used to build models in RITABackend. Two scenarios, `ngsim-i80` and `ngsim-us101`, are already integrated and tested. We are continuously working to incorporate more open-source datasets.
- *bubble* defines a special region in the roadway area to provide high quality and the most reactive traffic flow. Only social vehicles inside the bubble are controlled by the models from RITABackend. Before entering the bubble, the traffic is simply replaying the dataset, and after exiting the bubble, vehicles are controlled by IDM [38]. Bubble can be classified into two types, *moving* and *fixed*. The *moving* bubble is attached to and always covers the ego vehicle, while the *fixed* bubble is kept still in the specified positions.
- *interaction* configures the distribution of models that control social vehicles inside the bubble. Based on four typical interaction schemas in NGSIM I80 and US101, there are well-designed built-in options to choose from, e.g., `CommonLeftCutin`,

`CommonOnRamp`, `RareLeftCutin` and `RareOnRamp`. In ‘Common’ interaction, different models will be uniformly selected from the model zoo, while ‘Rare’ interaction uses more proportion of InfoGAIL models. Also, users are welcome to program their configuration by overriding the interaction handler. We provide examples in Appendix 11

- *guided_generation* controls whether guided initial states generation is used and the score function for guiding the diffusion process. For example, `None` means not using guided generation but uniformly sampling from datasets instead. `Stability` refers to built-in score function stands for generating states that make the benchmarked strategy get worse stability, according to our designed metric. We support score function reconstruction in configurable interfaces as well.

5.1 Environment Design

In this paper, we construct four typical interactive environments in a highway scenario to comprehensively assess the quality of the toolkit. We take open-source NGSIM I80 and US101 datasets for training and evaluation. All the environment ends until the desired interaction is completed or illegal termination events (e.g., collision) are triggered.

Task 1: Cut-in scenario. A moving bubble is created around the cut-in agent to take over surrounding vehicles using our reactive model. Considering different cut-in direction, we have left cut-in and right cut-in environments.

Task 2: Ramp scenario. Focusing on the classic ramp road structure in the highway scenario, we use the fixed bubble to replace the vehicles of the ramp lane and highway lane with the corresponding behavior model. We build on-ramp (enter the highway) and off-ramp (escape the highway) environments, respectively.

5.2 Generalized Traffic Flow Quality Measurement

In this subsection, we evaluate the quality of the interaction behavior and traffic flow, showing their high fidelity and diversity. In order to make a fair comparison, we extract human data with the same interaction and replace history vehicles under the same initial state.

5.2.1 Interaction Behavior Analysis. We first quantify how the reactive agent performs in the interaction scenario. In particular, we measure from three key dimensions: *time*, *time-to-collision (TTC)*, and *lateral speed*. *Time* can reveal the fluctuation during the interaction, and the other two dimensions show us more details about behavioral intensity and safety level.

To make reasonable analysis over *time*, we bring in the idea of Fourier analysis, mapping the time domain to the frequency domain for an overall view of the life cycle of an interaction. In detail, we conduct the fast Fourier transform (FFT) with 512 sample rates over lateral speed on trajectories and plot the envelope of them for each model, shown in Fig. 4a. Considering the area between the envelope and the frequency axis as a representation of the interaction distribution, we compare two quantitative evaluation metrics:

- *IoU*: Intersection area of model and human data / Union area.

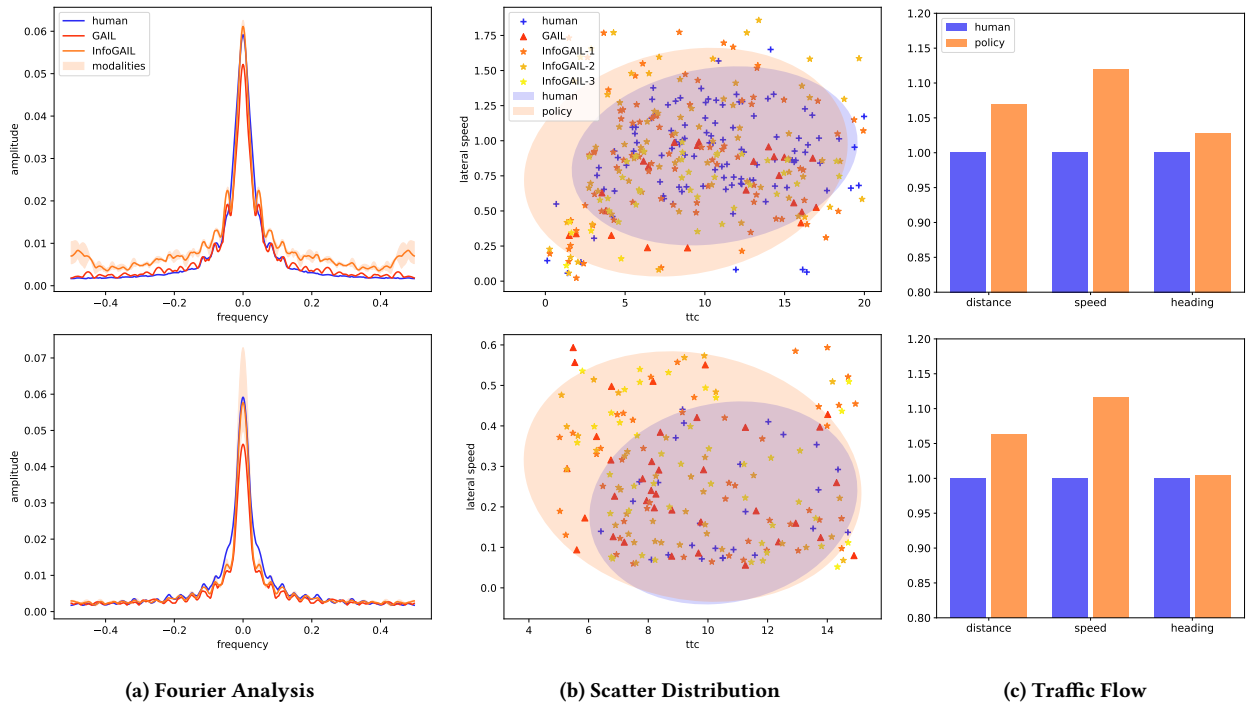


Figure 4: Benchmark Quality Measurement. The first row corresponds to the left cut-in scenario, and the second to the on-ramp scenario. For interaction, Fourier Analysis discusses lateral speed features over time, while Scatter Distribution focuses on the cut-in moment when the most vital interaction happens. For traffic, Traffic Flow quantifies the error of neighbors’ statistics between human data and policy-generalized data in an egocentric view.

- Coverage:

$$\frac{\sum_{f=-N}^N v_{\text{model}}(f)}{\sum_{f=-N}^N \max(v_{\text{model}}(f), v_{\text{human}}(f))},$$

where $v(f)$ is the amplitude at frequency f .

For analyzing *TTC* and *lateral speed*, we draw the scatter distribution at all cut-in moments in Fig. 4b. Assuming the data as Gaussian distribution, we further show the 95% confidence ellipse of human data and the combination of models (policy).

It is first and obviously noticed in Fig. 4a, both interactive models can cover almost all the frequency domain with high *IoU* (GAIL: 0.79, InfoGAIL: 0.73) and *Coverage* (GAIL: 0.91, InfoGAIL: 0.95), elucidating the interaction trajectories are realistic enough. For the InfoGAIL model, the shadow area indicates its modality difference, and we can find apparent diversity, especially in low and high frequency areas. Furthermore, in Fig. 4b, we find that the ellipse of reactive agents successfully matches most parts of human data distribution, showing its high fidelity. Additionally, the reactive agents occupy the nearby area of human distribution, which can be seen as a reasonable enhancement of interaction, showing the diversity of making rare cases.

5.2.2 Traffic Flow Analysis. We measure the traffic quality in a holistic view, i.e., qualify the traffic flow generated by multi-agent reactive agents. In particular, we use affordance [11] as the metric, which calculates metrics with neighbors in an ego-centric view.

Since interaction commonly happens between ego-agent and its neighbors, this metric is amenable for analyzing interactive traffic. Here we take *mean distance*, *speed*, *heading* of neighbor vehicles to describe traffic dynamically. With human data as baseline (normalized to 1), we plot statistical bar charts in Fig. 4c.

These statistics show clear evidence that the traffic around ego-agent is very similar to human data. The max error rate in both distance and heading $\leq 7\%$, speed $\leq 12\%$, elucidates that we recover high-fidelity trajectories beyond human data with reactivity and interaction.

6 BENCHMARK AND OPTIMIZATION OF DRIVING STRATEGIES

This section demonstrates two use cases of traffic flows generated by RITA. First, we show that the RITA traffic flow can be used to assess the performance of given driving strategies. Specifically, we demonstrate the results of using replay trajectories generated from guided traffic generation. Then, we demonstrate that the RITA environment successfully optimizes policy trained on history replay traffic flows.

6.1 Benchmark under RITA Traffic Flow

We benchmarked four popular AD solutions, including three machine learning algorithms, Behavior Cloning (BC), Generative Adversarial Imitation Learning (GAIL), Soft Actor-Critic [20] (SAC),

and a rule-based agent using keep-lane strategy based on the intelligent driver model (IDM).

We evaluate the safe-driving ability of algorithms under the interactive traffic we built above. Differing from quality measurement, here we design strong interaction patterns and let the test vehicle deal with constant active behavior from neighbors that affects its normal driving. In the left cut-in scenario, we make the right lane of ego-agent controlled by left cut-in models and the other two lanes controlled by multi-agent reactive agent (right cut-in similarly); in the on-ramp scenario, the ego-agent is placed at ramp lane with a continuous flow of merging vehicles controlled by interactive model while in off-ramp scenario we assigned reactive or off-ramp models for surrounding vehicles to build traffic.

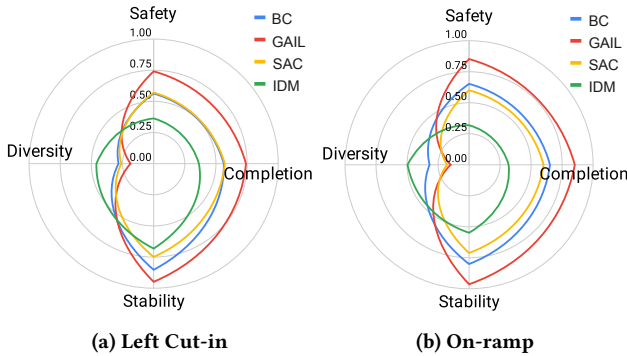


Figure 5: Benchmark Results. To keep consistency, we use the same metric as Fig. 3. Notice that we evaluate the safe-driving ability here, so Safety is numerically equal to Completion.

The results are depicted in Fig 5, where GAIL shows the best performance in the two tasks. The reason may be that GAIL can efficiently use expert training data and interact online with the simulator. On the contrary, IDM shows poor performance because of frequent interaction in the traffic, which the model itself cannot handle properly. Also, we observed that all algorithms perform better on fix-located traffic task *on-ramp*, which may imply interactive traffic with moving bubble has a more challenging dynamic to deal with.

Benchmark using Guided Generation. For the left cut-in environment, we conduct guided sampling of replay trajectories according to driving models, and evaluation results on these trajectories are shown in Tab. 1. The definition of *Stability* is the same as in Section 4.2, and *Distance Ratio* is the ratio of the actual distance traveled by the ego vehicle in the simulator to the distance traveled in the replay trajectory. The upper limit of the distance ratio is set to 1.

Specifically, we compare guided sampling (Guided) with two other sampling techniques, dataset sampling (Dataset) and normal sampling (Normal). Dataset sampling first samples a period of 128 time steps (12.8 seconds) from the dataset and randomly chooses one vehicle that appeared in this interval as the ego vehicle. Then the other 15 vehicles, which are most close to the ego vehicle at the first step, are chosen as social vehicles. Trajectories obtained by dataset sampling are also used to train the diffusion-based generative model.

Table 1: Comparisons of different types of sampling replay trajectories.

Metric	Sample Type	GAIL	SAC	BC
Stability	Dataset	0.911	0.811	0.822
	Normal	0.908	0.807	0.824
	Guided	0.861	0.719	0.775
Distance Ratio	Dataset	0.745	0.663	0.594
	Normal	0.734	0.653	0.591
	Guided	0.616	0.559	0.549

Table 2: Completion rates of two models before and after being finetuned under RITA traffic flow in the cut-in scenario.

	GAIL	GAIL-finetune	SAC	SAC-finetune
Replay	0.795	0.806	0.733	0.676
RITA	0.766	0.878	0.712	0.882

Normal sampling stands for a direct sample from the generative model. Guided sampling trains the scoring function network using the model performance on the dataset sampling trajectories, and its gradient is used to guide the generative model to produce samples resulting in the models’ low performance. For all three sampling methods, we sample 1000 trajectories for evaluation.

From Tab. 1, we observe that ego vehicles’ performance is similar when being evaluated on replay trajectories obtained by dataset sampling and normal sampling. This shows that the trajectories sampled by the generative model are similar to the dataset trajectories in evaluating the performance of the ego strategies. On the other hand, both stability and distance ratio evaluated on the guided generated trajectories are significantly lower than the others. In particular, the distance ratio of GAIL model is lowered by 16.1% with guided sampling, and the stability of SAC model is lowered by 10.9%.

6.2 Optimization under RITA Traffic Flow

To further claim the advantage of RITA, we take the history replay environment as our baseline and conduct optimization tasks. We first train two policies using SAC and GAIL, respectively, until convergence. Then we execute finetune with RITA interactive traffic flow and evaluate them under the history replay environment and RITA environment.

The result can be seen in Table 2. It suggests two significant facts: (1) Policy trained by history replay shows relatively poor performance in the RITA environment, indicating that it can hardly handle a dynamic environment with realistic human response. (2) Policy finetuned by RITA achieves high performance in both evaluations, implying that RITA can output a more robust policy than static human replay data. Given that surrounding vehicles can make reasonable responses even if the policy itself deviates from the dataset trajectory in the RITA environment, it somehow means that collisions happening in the RITA environment are more unacceptable. The performance drop may suggest a not small loss

in interaction ability and will cause agent collision when facing similar real-world situations.

7 RELATED WORK

7.1 Microscopic Traffic Simulation

Unlike macroscopic traffic simulation, which models average vehicle dynamics like traffic density, microscopic traffic simulation separately models each vehicle and its dynamics, playing a critical role in optimizing self-driving strategies in simulators. Most traffic simulators or benchmarks use heuristic-based models to simulate the background traffic [17, 19, 38], e.g., following the lane and avoiding head-on collisions [15]. Since human driving behaviors are hard to define completely with heuristic rules, these methods lack the ability to model complex multi-vehicle interactions. SimNet [3] is similar to our approach in using a data-driven approach to obtain models for social vehicle control. However, the control models in SimNet are trained in an offline manner, which is more sensitive to distribution shifts.

Microscopic traffic simulation solutions in autonomous driving simulators need to offer easy-to-use interfaces to allow users to specify specific characteristics of the traffic flow. However, most traffic generation algorithms do not provide such interfaces [2, 6], so the additional design is required when incorporating into simulators. RITA, as a complete microscopic traffic generation framework independent of the simulator, integrates the interface for traffic definition in RITAKit.

Another group of studies on microscopic traffic simulation focus on generating traffic flows that make self-driving vehicles perform poorly. Ding et.al. [14] propose to generate safety-critical scenarios by sampling from a pre-designed probability graphic model, where conditional probabilities are optimized via the policy gradient. Such optimization with reinforcement learning does not utilize real datasets, and the generated scenarios may lack fidelity. AdvSim [39] conducts black-box adversarial attacks on real-world trajectories by adding perturbations to vehicles’ behaviors. However, random perturbations may drive the final generated samples away from the true data distribution. Although the aforementioned corner-case generation methods can be used to evaluate the worst performance of a strategy, such unrealistic scenarios violate the fidelity requirement of RITA. Instead, RITA provides an adversarial sampling of scenarios given the current strategy while constraining the generated scenarios to stay within the real data distribution.

Table 3: Comparison of microscopic traffic flows in driving simulations. Sim, bench, comp are shorts for simulator, benchmark, component respectively.

Name	Data-driven Models	Configurable Interface	Adversarial Generation	Type
CARLA [15]	✗	✓	✗	Sim
SMARTS [43]	✗	✓	✗	Sim
BARK [5]	✓	✓	✗	Bench
NuPlan [10]	✓	✓	✗	Bench
SimNet [3]	✓	✗	✗	Comp
AdvSim [39]	✗	✗	✓	Comp
RITA (Ours)	✓	✓	✓	Comp

We compare microscopic traffic flows in existing driving simulation literature from three aspects in Tab. 3. Specifically, we judge whether these traffic flows are generated by data-driven driving models, provide a configurable interface for controllable generation, and support generating specific rare-case traffic.

7.2 Human Behavior Modeling

To more accurately evaluate the performance of the autonomous driving model in real traffic, we choose to deploy social vehicle models that imitate human drivers in the simulator. This requires us to adopt a practical approach to human behavior modeling. Human behavior modeling is becoming a trending research direction in the field of human-robot interaction (HRI) and has been used for various purposes. A direct motivation is to obtain control policies by imitating human data and deploying the imitated models on robots or autonomous vehicles [6, 12, 23]. Other than directly using human behavior models to control the robots, these models can also help robots make decisions by predicting the actions of humans who interact with them [29, 33]. Moreover, if learned human models are conditioned on the robots’ actions, they can be used to reason future human responses to robot behavior, which enables the robots to proactively shape or guide human behaviors [16, 37]. Another goal of building human behavior models is to build more realistic simulators that can better access or improve the model performances in human-robot interactions without real interaction with humans [10, 34]. RITA aims to accomplish this goal in autonomous driving tasks and adopts several adversarial imitation learning methods to build human behavior models. Since human behavior modeling is attracting more and more research attention, more advanced human modeling techniques can be continuously incorporated into the RITA framework.

8 CONCLUSIONS

This paper presents RITA, a framework for generating high-quality traffic flow in a driving simulator. RITA contains several components, first is RITABackend, which learns vehicle control and static trajectories generation models from real-world datasets; besides, built on top of RITABackend, RITAKit provides an easy-to-use interface to customize the traffic flow. Combining these two modules, RITA can deliver traffic flow with high fidelity, diversity, and controllability. Under RITA, we design two benchmark tasks with highly interactive traffic flow. Under these two tasks, we conduct experiments to show the high quality of generated traffic flows from multiple perspectives. Also, we demonstrate two use cases of RITA: evaluating the performance of existing driving strategies and fine-tuning those driving strategies.

We believe that RITA will be integrated into existing simulators, and we look forward to making RITA a standard component of driving simulators.

REFERENCES

- [1] Saurabh Arora and Prashant Doshi. 2021. A survey of inverse reinforcement learning: Challenges, methods and progress. *Artificial Intelligence* 297 (2021), 103500.
- [2] Mayank Bansal, Alex Krizhevsky, and Abhijit Ogale. 2018. Chauffeurnet: Learning to drive by imitating the best and synthesizing the worst. *arXiv preprint arXiv:1812.03079* (2018).

- [3] Luca Bergamini, Yawei Ye, Oliver Scheel, Long Chen, Chih Hu, Luca Del Pero, Blażej Osiński, Hugo Grimmer, and Peter Ondruska. 2021. Simnet: Learning reactive self-driving simulations from real-world observations. In *2021 IEEE International Conference on Robotics and Automation (ICRA)*. IEEE, 5119–5125.
- [4] Luca Bergamini, Yawei Ye, Oliver Scheel, Long Chen, Chih Hu, Luca Del Pero, Blażej Osiński, Hugo Grimmer, and Peter Ondruska. 2021. SimNet: Learning Reactive Self-driving Simulations from Real-world Observations. In *2021 IEEE International Conference on Robotics and Automation (ICRA)*. 5119–5125. <https://doi.org/10.1109/ICRA48506.2021.9561666>
- [5] Julian Bernhard, Klemens Esterle, Patrick Hart, and Tobias Kessler. 2020. BARK: Open behavior benchmarking in multi-agent environments. In *2020 IEEE/RSJ International Conference on Intelligent Robots and Systems (IROS)*. IEEE, 6201–6208.
- [6] Raunak Bhattacharyya, Blake Wulfe, Derek Phillips, Alex Kuefler, Jeremy Morton, Ransalu Senanayake, and Mykel Kochenderfer. 2020. Modeling human driving behavior through generative adversarial imitation learning. *arXiv preprint arXiv:2006.06412* (2020).
- [7] Raunak P Bhattacharyya, Derek J Phillips, Changliu Liu, Jayesh K Gupta, Katherine Driggs-Campbell, and Mykel J Kochenderfer. 2019. Simulating emergent properties of human driving behavior using multi-agent reward augmented imitation learning. In *2019 International Conference on Robotics and Automation (ICRA)*. IEEE, 789–795.
- [8] Raunak P Bhattacharyya, Derek J Phillips, Blake Wulfe, Jeremy Morton, Alex Kuefler, and Mykel J Kochenderfer. 2018. Multi-agent imitation learning for driving simulation. In *2018 IEEE/RSJ International Conference on Intelligent Robots and Systems (IROS)*. IEEE, 1534–1539.
- [9] Raunak P. Bhattacharyya, Derek J. Phillips, Blake Wulfe, Jeremy Morton, Alex Kuefler, and Mykel J. Kochenderfer. 2018. Multi-Agent Imitation Learning for Driving Simulation. In *2018 IEEE/RSJ International Conference on Intelligent Robots and Systems (IROS)*. 1534–1539. <https://doi.org/10.1109/IROS.2018.8593758>
- [10] Holger Caesar, Juraj Kabzan, Kok Seang Tan, Whye Kit Fong, Eric Wolff, Alex Lang, Luke Fletcher, Oscar Beijbom, and Sammy Omari. 2021. nuplan: A closed-loop ml-based planning benchmark for autonomous vehicles. *arXiv preprint arXiv:2106.11810* (2021).
- [11] Chenyi Chen, Ari Seff, Alain Kornhauser, and Jianxiong Xiao. 2015. DeepDriving: Learning Affordance for Direct Perception in Autonomous Driving. In *Proceedings of the IEEE International Conference on Computer Vision (ICCV)*.
- [12] Felipe Codevilla, Matthias Müller, Antonio López, Vladlen Koltun, and Alexey Dosovitskiy. 2018. End-to-end driving via conditional imitation learning. In *2018 IEEE international conference on robotics and automation (ICRA)*. IEEE, 4693–4700.
- [13] Pim De Haan, Dinesh Jayaraman, and Sergey Levine. 2019. Causal confusion in imitation learning. *Advances in Neural Information Processing Systems* 32 (2019).
- [14] Wenhao Ding, Baiming Chen, Minjun Xu, and Ding Zhao. 2020. Learning to collide: An adaptive safety-critical scenarios generating method. In *2020 IEEE/RSJ International Conference on Intelligent Robots and Systems (IROS)*. IEEE, 2243–2250.
- [15] Alexey Dosovitskiy, German Ros, Felipe Codevilla, Antonio Lopez, and Vladlen Koltun. 2017. CARLA: An open urban driving simulator. In *Conference on robot learning*. PMLR, 1–16.
- [16] Anca D Dragan, Shira Bauman, Jodi Forlizzi, and Siddhartha S Srinivasa. 2015. Effects of robot motion on human-robot collaboration. In *2015 10th ACM/IEEE International Conference on Human-Robot Interaction (HRI)*. IEEE, 51–58.
- [17] Mohamed Elsayed, Kimia Hassanzadeh, Nhat M Nguyen, Montgomery Alban, Xiru Zhu, Daniel Graves, and Jun Luo. 2020. ULTRA: A reinforcement learning generalization benchmark for autonomous driving. (2020).
- [18] Scott Ettinger, Shuyang Cheng, Benjamin Caine, Chenxi Liu, Hang Zhao, Sabeek Pradhan, Yuning Chai, Ben Sapp, Charles R Qi, Yin Zhou, et al. 2021. Large scale interactive motion forecasting for autonomous driving: The waymo open motion dataset. In *Proceedings of the IEEE/CVF International Conference on Computer Vision*. 9710–9719.
- [19] Peter G Gipps. 1981. A behavioural car-following model for computer simulation. *Transportation Research Part B: Methodological* 15, 2 (1981), 105–111.
- [20] Tuomas Haarnoja, Aurick Zhou, Pieter Abbeel, and Sergey Levine. 2018. Soft Actor-Critic: Off-Policy Maximum Entropy Deep Reinforcement Learning with a Stochastic Actor. In *Proceedings of the 35th International Conference on Machine Learning (Proceedings of Machine Learning Research, Vol. 80)*, Jennifer Dy and Andreas Krause (Eds.). PMLR, 1861–1870.
- [21] John Halkias and James Colyar. 2006. Next generation simulation fact sheet. *US Department of Transportation: Federal Highway Administration* (2006).
- [22] Jonathan Ho and Stefano Ermon. 2016. Generative adversarial imitation learning. *Advances in neural information processing systems* 29 (2016).
- [23] Chien-Ming Huang, Maya Cakmak, and Bilge Mutlu. 2015. Adaptive Coordination Strategies for Human-Robot Handovers.. In *Robotics: science and systems*, Vol. 11. Rome, Italy, 1–10.
- [24] Parth Kothari, Christian Perone, Luca Bergamini, Alexandre Alahi, and Peter Ondruska. 2021. Drivervgym: Democratizing reinforcement learning for autonomous driving. *arXiv preprint arXiv:2111.06889* (2021).
- [25] Daniel Krajzewicz, Georg Hertkorn, Christian Rössel, and Peter Wagner. 2002. SUMO (Simulation of Urban MObility)-an open-source traffic simulation. In *Proceedings of the 4th middle East Symposium on Simulation and Modelling (MESM2002)*. 183–187.
- [26] Alex Kuefler, Jeremy Morton, Tim Wheeler, and Mykel Kochenderfer. 2017. Imitating driver behavior with generative adversarial networks. In *2017 IEEE Intelligent Vehicles Symposium (IV)*. IEEE, 204–211.
- [27] Yunzhu Li, Jiaming Song, and Stefano Ermon. 2017. Infogail: Interpretable imitation learning from visual demonstrations. *Advances in Neural Information Processing Systems* 30 (2017).
- [28] Minghuan Liu, Tairan He, Minkai Xu, and Weinan Zhang. 2020. Energy-based imitation learning. *arXiv preprint arXiv:2004.09395* (2020).
- [29] Jim Mainprice, Rafi Hayne, and Dmitry Berenson. 2016. Goal set inverse optimal control and iterative replanning for predicting human reaching motions in shared workspaces. *IEEE Transactions on Robotics* 32, 4 (2016), 897–908.
- [30] Blażej Osiński, Piotr Miłoś, Adam Jakubowski, Paweł Zięcina, Michał Martyniak, Christopher Galias, Antonia Breuer, Silviu Homoceanu, and Henryk Michalewski. 2020. CARLA Real Traffic Scenarios—novel training ground and benchmark for autonomous driving. *arXiv preprint arXiv:2012.11329* (2020).
- [31] Guodong Rong, Byung Hyun Shin, Hadi Tabatabaee, Qiang Lu, Steve Lemke, Márton Mozeiko, Eric Boise, Geehoon Uhm, Mark Gerow, Shalin Mehta, et al. 2020. Lgsvl simulator: A high fidelity simulator for autonomous driving. In *2020 IEEE 23rd International conference on intelligent transportation systems (ITSC)*. IEEE, 1–6.
- [32] Stéphane Ross and Drew Bagnell. 2010. Efficient reductions for imitation learning. In *Proceedings of the thirteenth international conference on artificial intelligence and statistics*. 661–668.
- [33] Wilko Schwarting, Alyssa Pierson, Javier Alonso-Mora, Sertac Karaman, and Daniela Rus. 2019. Social behavior for autonomous vehicles. *Proceedings of the National Academy of Sciences* 116, 50 (2019), 24972–24978.
- [34] Jing-Cheng Shi, Yang Yu, Qing Da, Shi-Yong Chen, and An-Xiang Zeng. 2019. Virtual-taobao: Virtualizing real-world online retail environment for reinforcement learning. In *Proceedings of the AAAI Conference on Artificial Intelligence*, Vol. 33. 4902–4909.
- [35] Jiaming Song, Hongyu Ren, Dorsa Sadigh, and Stefano Ermon. 2018. Multi-agent generative adversarial imitation learning. *Advances in neural information processing systems* 31 (2018).
- [36] Yang Song, Jascha Sohl-Dickstein, Diederik P Kingma, Abhishek Kumar, Stefano Ermon, and Ben Poole. 2020. Score-based generative modeling through stochastic differential equations. *arXiv preprint arXiv:2011.13456* (2020).
- [37] Stefanie Tellex, Ross Knepper, Adrian Li, Daniela Rus, and Nicholas Roy. 2014. Asking for help using inverse semantics. (2014).
- [38] Martin Treiber, Ansgar Hennecke, and Dirk Helbing. 2000. Congested traffic states in empirical observations and microscopic simulations. *Physical review E* 62, 2 (2000), 1805.
- [39] Jingkan Wang, Ava Pun, James Tu, Sivabalan Manivasagam, Abbas Sadat, Sergio Casas, Mengye Ren, and Raquel Urtasun. 2021. Advsim: Generating safety-critical scenarios for self-driving vehicles. In *Proceedings of the IEEE/CVF Conference on Computer Vision and Pattern Recognition*. 9909–9918.
- [40] Tian Xu, Ziniu Li, and Yang Yu. 2020. Error bounds of imitating policies and environments. *Advances in Neural Information Processing Systems* 33 (2020), 15737–15749.
- [41] Wei Zhan, Liting Sun, Di Wang, Haojie Shi, Aubrey Clause, Maximilian Nammann, Julius Kümmerle, Hendrik Königshof, Christoph Stiller, Arnaud de La Fortelle, and Masayoshi Tomizuka. 2019. INTERACTION Dataset: An International, Adversarial and Cooperative motion Dataset in Interactive Driving Scenarios with Semantic Maps. *arXiv:1910.03088 [cs, eess]* (2019).
- [42] Weinan Zhang, Zhengyu Yang, Jian Shen, Minghuan Liu, Yimin Huang, Xing Zhang, Ruiming Tang, and Zhenguo Li. 2021. Learning to Build High-fidelity and Robust Environment Models. *ECMLPKDD* (2021).
- [43] Ming Zhou, Jun Luo, Julian Villeda, Yaodong Yang, David Rusu, Jiayu Miao, Weinan Zhang, Montgomery Alban, Iman Fadakar, Zheng Chen, et al. 2020. Smarts: Scalable multi-agent reinforcement learning training school for autonomous driving. *arXiv preprint arXiv:2010.09776* (2020).

APPENDIX

9 SIMULATION SPACE

9.1 Observation Space

To let models be generalized in different maps, we collect information from three main aspects in egocentric coordinates: [*Ego dynamics*, *Lane observation*, *Neighbor observation*].

9.1.1 Ego dynamics. Ego dynamics choose the absolute value to represent ego vehicle attributes. Here we simply use *linear velocity* since heading and position are relative amounts changing with the map.

9.1.2 Lane observation. In SMARTS, the simulator produces a list of equally spaced points in the centerline of lanes on the map, called waypoints. Each waypoint has its position and heading. Therefore by calculating relative data between the nearest waypoint and the ego vehicle, we can locate our position on the map. We here calculate the relative position and heading of the ego, left, and right lane between agent and nearest waypoint.

9.1.3 Neighbor observation. We divided neighbor vehicles into eight areas according to their relative position, illustrated in Fig 6. The first letter indicates its position: ['B'ottom, 'M'iddle, 'T'op] while the second indicates its lane: ['L'eft, 'M'iddle, 'R'ight]. We calculate the relative position, heading, and speed for each neighbor.

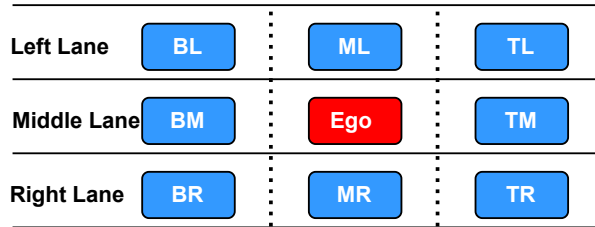


Figure 6: Neighbor Position. The first letter indicates the neighbor’s relative position, while the second indicates its lane.

9.2 Action Space

We here take continuous 2-dimensional *linear acceleration* a_l and *angular velocity* w_a as our action space. As SMARTS deploys a dynamic vehicle model with physical constraints and we want to make reasonable behavior compared to the NGSIM dataset, we here make corresponding limitation for $a_l \in [-3.0, 3.0]m/s^2$ and $w_a \in [-2.0, 2.0]rad/s$.

10 MODEL ZOO

The tabular model zoo used for constructing interaction scenarios is shown in Table 4. We have trained common reactive models as well as models dealing with specific interactions.

Algorithm	Training Scenarios	Model
GAIL	left cut-in, right cut-in, on-ramp, off-ramp	left cut-in, right cut-in, on-ramp, off-ramp
MAGAIL	all scenarios	reactive
InfoGAIL	left cut-in, right cut-in, on-ramp, off-ramp	left cut-in, right cut-in, on-ramp, off-ramp [$c = 1, 2, 3$]

Table 4: Benchmark Model Zoo. The entire model zoo is trained from the open-sourced dataset. For GAIL and InfoGAIL, each interaction scenario trains a corresponding model. For MAGAIL, we get a general reactive model using the parameter-sharing technique. We can change the modality of InfoGAIL model by assigning a different value of latent variable c .

11 SCENARIO GENERATION EXAMPLES

We give extra code examples for creating specific interactive traffic following the scheme in the main paper. While in the main paper, we give a brief introduction with built-in configuration, here we make simple reconstruction to help users understand the RITA structure. It is welcome to override the interaction handler and other interfaces to formulate wanted scenario.

```
1 ScenarioMaker(  
2     scenario = "ngsim-us101",  
3     bubble = Bubble(  
4         type='moving',  
5         zone=Rectangle(40,20)),  
6     interaction = CutinHandler(  
7         assign_type='common',  
8         cutin_direction='left',  
9         checker='lane_change',  
10    ),  
11    guided_generation = DiffusionGenerator(  
12        guided_mode='Distance',  
13        target=policy,  
14    ),  
15 )
```

```
1 ScenarioMaker(  
2     scenario = "ngsim-i80",  
3     bubble = Bubble(  
4         type='fixed',  
5         position=(140,0),  
6         zone=Rectangle(110,15)),  
7     interaction = OnRampHandler(  
8         assign_type='rare',  
9         checker = RampChecker(  
10            ramp_lane='E3',  
11            main_lane='gneE01'  
12        )  
13    ),  
14    guided_generation = "None",  
15 )
```

Left Cut-in Scenario Example

On-ramp Scenario Example

Figure 7: Code Example with Simple Reconstruction. A basic *InteractionHandler* require two arguments: *assign_type* for interactive model assignment, *checker* for interaction behavior identification. A basic *DiffusionGenerator* needs to offer *guided_mode* (i.e. score function) to train $\mathcal{J}(x)$ and the *target* model for simulation.

12 ALGORITHM PARAMETERS

Here we describe basic information about benchmarked algorithm implementation. Algorithms used in benchmark and optimization experiments share the same setting.

12.1 Rule-Based Model

The model from the SMARTS agent zoo is controlled by IDM. We use a keep-lane agent as we do not ask the model to do active interaction behavior but to make reasonable responses under it.

12.2 Machine Learning Model

To conduct as fair a comparison as possible, we make all the algorithms have the same state-action space and policy network structure. We choose five random seeds for each algorithm and record their average performance. We share necessary algorithm parameters in Table 5.

13 ADDITIONAL RESULTS

Here we put the right cut-in scenario and off-ramp scenario results. To achieve high fidelity, the data-driven model zoo must access adequate qualified interaction data to learn good policy, which means the lack of desired data harms the performance of model and the simulated scenario. The training data of the right cut-in scenario only accounts for 1/6 of the total cut-in data. And for the off-ramp scenario, about 95% of data follows the lane and not producing meaningful interaction, making it hard to create high-quality traffic flow.

13.1 Model Performance

Because of the data limitation mentioned above, performance in Fig 8 not reflects ideal situations in both scenarios. The right cut-in performance drops compared to the left cut-in, while off-ramp performance achieves abnormally high results due to interaction trajectories' absence in data.

13.2 Interaction Traffic Analysis

The interaction quality suffers from the same declination in model performance, which can be seen in Fig 9a and Fig 9b, where the average *IoU* and *Coverage* decreased and scatter distribution matches poorly with human data. However, the traffic flow quality shown in Fig 9c remains stable as the reactive ability not be hurt.

Table 5: Algorithm Parameters

BC	parameters
Network	MLP
Hidden Size	256
Hidden Layers	3
Batch Size	1024
Learning Rate	0.0003
Loss Function	MSE

GAIL	parameters
Network	MLP
Policy Hidden Size	256
Policy Hidden Layers	3
Discriminator Hidden Size	64
Discriminator Hidden Layer	2
Batch Size	256
Policy Learning Rate	0.0003
Discriminator Learning Rate	0.0003
Policy Trainer	SAC

SAC	parameters
Network	MLP
Policy Hidden Size	256
Policy Hidden Layers	3
Batch Size	256
Alpha	0.2
Policy Learning Rate	0.0003
Q Learning Rate	0.0003
Reward	Travel Distance

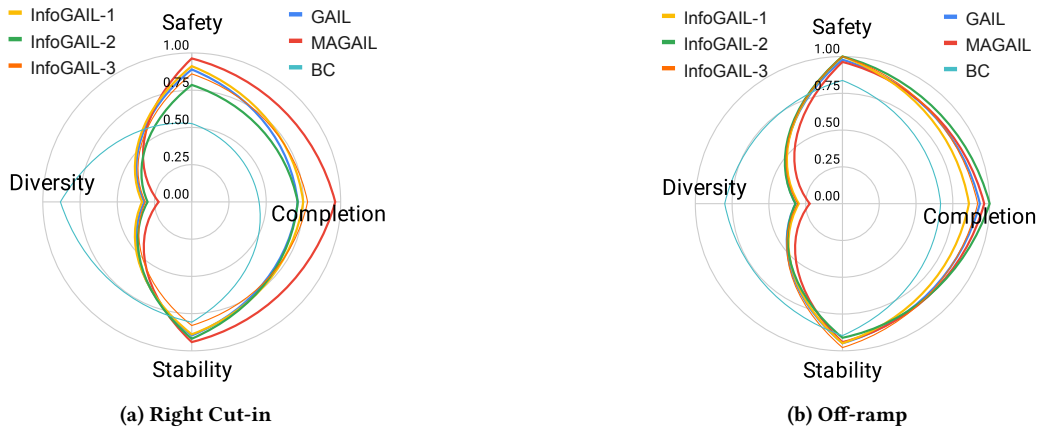


Figure 8: Model Performance.

13.3 Benchmark Results

In fig 10, we still benchmark algorithms in right cut-in and off-ramp scenarios. In the right cut-in scenario, GAIL shows even more performance advantage compared to the left cut-in scenario, as it can make use of both expert data and simulation results. We have to design a simple task for the off-ramp scenario due to the aforementioned model limitation. Here we find IDM achieves the best performance, as it can execute lane-following tasks flawlessly.

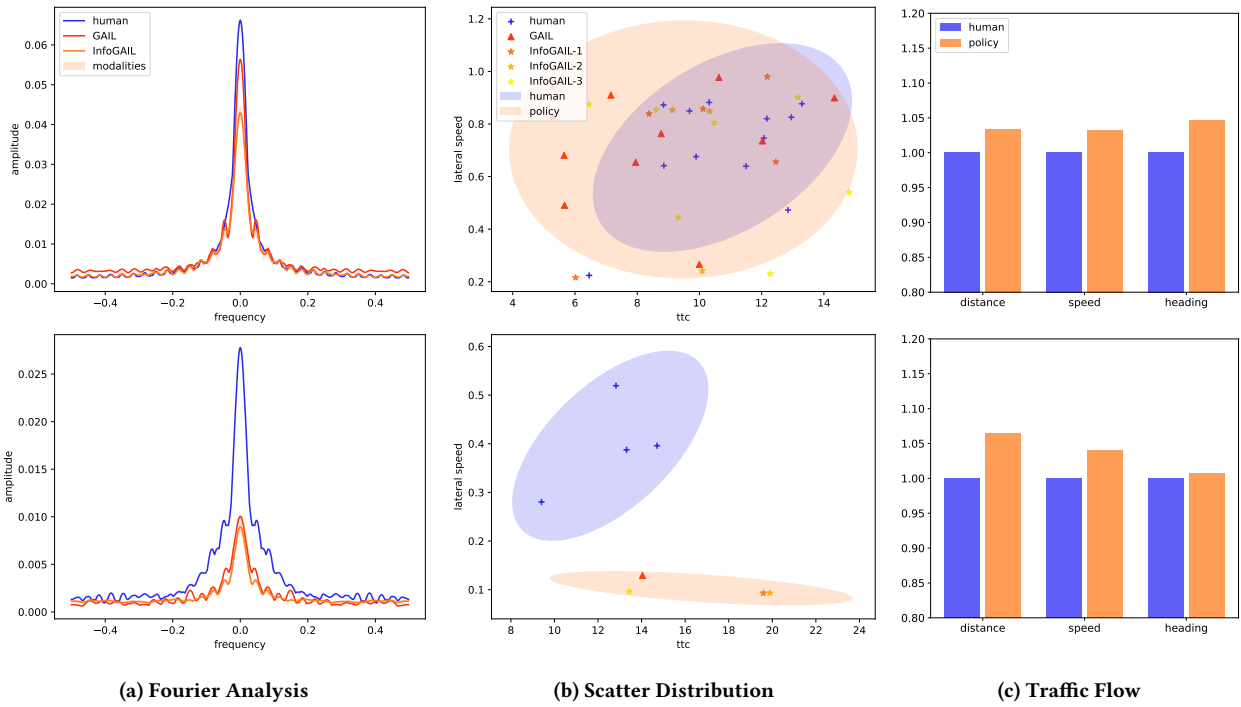


Figure 9: Benchmark Quality Measurement. The first row corresponds to the right cut-in scenario, and the second to the off-ramp scenario.

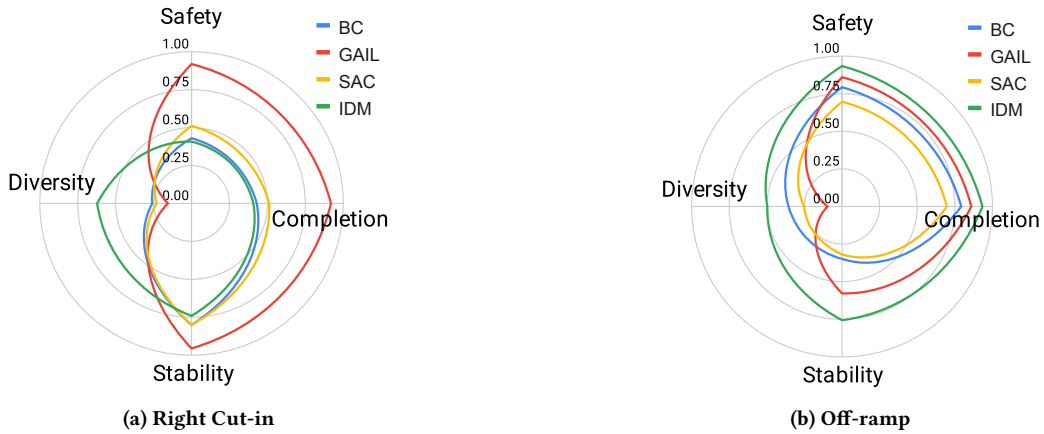


Figure 10: Benchmark Results.